



# Physical characterization of fine particulate matter inside the public transit buses fueled by biodiesel in Toledo, Ohio

Kaushik K. Shandilya<sup>1</sup>, Ashok Kumar\*

Department of Civil Engineering, The University of Toledo, 2801 W. Bancroft Street, Toledo, OH 43606-3390, United States

## ARTICLE INFO

### Article history:

Received 16 January 2011

Received in revised form 9 March 2011

Accepted 21 March 2011

Available online 29 March 2011

### Keywords:

Single inhalable particle  
Morphology  
Physical characterization  
Urban-public transit bus  
Biodiesel

## ABSTRACT

This study presents the physical characteristics of fine particulate matter (PM) collected inside the urban-public transit buses in Toledo, OH. These buses run on 20% biodiesel blended with ultra-low sulfur diesel (ULSD) (B20). For risk analysis, it is crucial to know the modality of the size distribution and the shape factor of PM collected inside the bus. The number-size distribution, microstructure, and aspect ratio of fine PM filter samples collected in the urban-public transit buses were measured for three years (2007–2009), using an environmental scanning electron microscope (ESEM) coupled with energy dispersive X-ray spectrometry (EDX). Only the reproducible results from repeated experiments on ESEM and size distribution obtained by the GRIMM dust monitor were used in this study. The size distribution was found bi-modal in the winter and fall months and was primarily uni-modal during spring and summer. The aspect ratio for different filter samples collected inside the bus range from 2.4 to 3.6 in average value, with standard deviation ranging from 0.9 to 7.4. The square-shaped and oblong-shaped particles represent the single inhalable particle's morphology characteristics in the air of the Toledo transit buses.

© 2011 Elsevier B.V. All rights reserved.

## 1. Introduction

In some societies, there is a great deal of driving between work and home. This mobility often takes place inside a motor vehicle, which can be problematic because of all of the particulates that build up [1]. Depending on how large the particles are, people inside a vehicle can become sick from inhaling these particles. Because of this risk, there is a need to improve scientific knowledge and information on the size, morphology, and microstructure of particles contributing to the indoor air of urban-public transit buses. This is done so that the extent of particle influence on passenger health can be better estimated in future risk studies. The indoor particulate matter concentration depends on many factors like the load conditions, rated engine power, the quality of diesel fuel used for blending, the type of engine, and operation temperature, but individual particle studies are not affected by those factors, air changes per hour, indoor environment [2]. The explanation to this fact is that indoor particulate matter concentration is a macro property of the pollutant while individual particles are micro properties of the particulate mass present at a certain time.

The size distribution is one of the most important physical characteristics of particulate matter, as it can reveal the source information and health risk [3]. A mode is defined as a peak in the PSD that can also be described by a lognormal function for the number size distribution of PM [4]. In context, a mode mostly represents a category of particles formed by the same processes [5]. The ultra-fine mode is near 0.1  $\mu\text{m}$  and the coarse mode is beyond 0.3  $\mu\text{m}$  [6]. The physical dimensions of the particles are used to categorize the particles which largely influence the deposition of particles in the lung and then increase the oxidative stress on the lung tissues [7]. Moreover, identifying particle size distribution (PSD) modes by presence, location, and particle boundary govern exposure and risk assessment. These factors also help in understanding particle formation mechanisms [8]. Furthermore, modes could serve as direct pointers to appropriate mitigation strategies for lowering environmental and human health effects [9].

In the absence of shape factor, most researchers assume all the particles as spherical when converting the particle number to particle mass, which introduces error to the risk calculations [10]. Aspect ratio is defined by the ratio of particle length and thickness [11]. To the best of our knowledge, this is the first study that provides a vast database for shape factors for a large number of particles collected inside a bus over a period of three years.

The analytical scanning electron microscope has been frequently used for the qualitative characterization of aerosols in the past [12]. Coupled with the new National Ambient Air Quality Standards (NAAQS), particulate health studies have generated

\* Corresponding author. Tel.: +1 419 530 8120/8136.

E-mail addresses: [kshandi@rockets.utoledo.edu](mailto:kshandi@rockets.utoledo.edu) (K.K. Shandilya), [akumar@utoledo.edu](mailto:akumar@utoledo.edu) (A. Kumar).

<sup>1</sup> Tel.: +1 419 464 1599.

greater interest in analytical techniques capable of measuring the size and morphology of individual aerosol particles [13–15]. The shapes of single inhalable particles collected inside an urban-transit bus fueled by biodiesel have been reported by Shandilya and Kumar [14,15]. In this study, an environmental electron microscopy technique was used to characterize—from a physical point of view—the ‘coarse’ and ‘fine’ components of airborne PM collected inside an urban-public transit bus. As manual counting would be extremely time-consuming, an automated particle analysis program for SEM/EDX was used in this biodiesel bus study.

As the world struggles to achieve a better environment and sustainable growth, many people visualize biodiesel as an alternative fuel to those that are frequently used. However, PM physical characteristics such as particle size distribution, aspect ratio, and shape factors are not available for indoor environments in biodiesel-fueled urban-public transit buses around the world. The scope of this study does not include the nano-sized particles, since this study was not designed to collect nano-sized particles. The purpose of this research is to improve scientific information on the particle morphology and microstructure of engine-emitted particulates, as they should be useful to further assess the indoor health impact of particulates. The objective of this study is to establish an understanding of the physical characteristics of particles collected inside this type of transit bus, with respect to the seasonal changes that occur in the Toledo area.

## 2. Materials and methods

### 2.1. Study site

The city of Toledo is located in the northwest of the state of Ohio, USA. Like several other cities in the Great Lakes region, Toledo experiences a lake-moderated humid continental climate, characterized by four distinct seasons varying significantly in temperature and precipitation:

- Spring: March, April, May
- Summer: June, July, August
- Fall: September, October, November
- Winter: December, January, February

Toledo is the primary market city for northwest Ohio, a region of nine counties with a population of one million. As such, there is a high concentration of retail establishments and medical facilities in Toledo. As mentioned in the transportation energy and carbon footprints of the 100 largest U.S. Metropolitan areas [16], the Toledo city council is taking many steps to reduce the carbon footprints. In this endeavor, all TARTA buses, the city of Toledo trucks, and The University of Toledo buses are now running on biodiesel. The Toledo area regional transportation agency (TARTA) has an annual passenger mileage of 22 million, so the majority of the population is affected by the shift from petroleum diesel to biodiesel.

### 2.2. Sampling

The particulate matter samples were collected inside urban transit buses operated by TARTA on Route 20, as shown in Fig. 1 [15]. The GRIMM dust monitor 1.108 was used at 1.2L/min with a size range of 0.3–20  $\mu\text{m}$  (aerodynamic diameter) using 47 mm polycarbonate filters (GRIMM Inc.) with 0.3  $\mu\text{m}$  pores for the microscopic analysis. Each sample was collected for the period of an ordinary day's condition inside heating, ventilating, and air conditioning (HVAC)-equipped B20-fueled buses. The sampling periods are given in Table 1. The above samples were collected in a homogeneous environment inside the bus and the sampling was

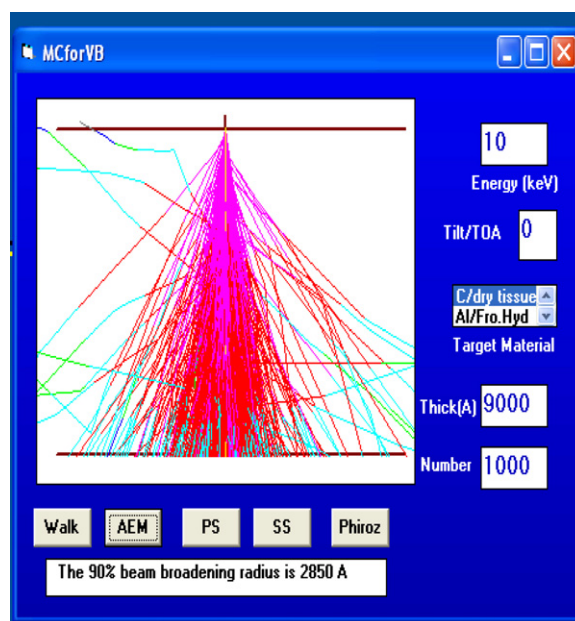


Fig. 1. Monte Carlo simulations for 1  $\mu\text{m}$  particles at beam energy of 10 keV showing the penetration by the electron beams into the substrate for the smaller particles.

continuous, using the same filter. The samples were stored in a deep freezer before any analysis was carried out.

### 2.3. SEM/EDX detection

The whole filter paper was mounted on a smooth Cu-alloy stub for the SEM analysis. The analysis of the particle samples was performed by a QUANTA 3D with gaseous backscattering secondary electron detector (GBSD) equipped with an EDX system for X-ray microanalysis by energy dispersion spectrometry. For the automated image and data collection and analysis, the electron beam of 10 keV at 67 Pa was focused on one spot to collect an EDX spectrum. The particles are automatically segmented and detected by an increase in the secondary electron (SE) and in the back-scattered electron (BSE) video signal above a preset video threshold [17]. This was set in such a manner so that the particles could be identified correctly as individual particles. The beam was moved to the next particle in the spot and the process was repeated until the entire spot was analyzed. After analyzing all the particles in a field, the stage was moved to the location of the next field and SEM/EDX repeated the entire process again until at least 20 fields were analyzed. After the initial setup, all the steps described above were completed with the data saved automatically. For each particle, the average, maximum, and Feret diameters were determined for the area and perimeter. It should be noted that the three dimensional morphology cannot be investigated by SEM and more ESEM/EDX specifications are mentioned previously by the authors [14,15].

The Monte Carlo simulations for 1  $\mu\text{m}$  particles at beam energy of 10 keV were performed to ensure that the electron beam detection of particle boundary for smaller particles is accurate (Fig. 1). Airborne particles are typically very fine (<3  $\mu\text{m}$ ) and the minimum size used for the automated analysis was 0.19  $\mu\text{m}$ . Particles of this size and composition will allow electrons to pass through the particle into the substrate/filter. The chemical characterization was not undertaken during this study, so substrate penetration and contribution are not matters of concern.

**Table 1**  
Sampling periods, particles counted, aspect ratio, and size distribution.

MM/YY	# Particles counted in different experiment ( <i>p</i> -value in percent)				Aspect ratio	Size distribution	
	The GRIMM	I	II	III		Modality	Peaks
Jan-07	111,059,814 ( $p_{1G} = 18.4$ ; $p_{2G} = 21.7$ ; $p_{3G} = 18.4$ )	<b>6172</b> ( $p_{12} = 5.7$ ; $p_{13} = 5.7$ )	2615 ( $p_{23} = 18.4$ )	914	$3.9 \pm 5.9$	Uni-Modal	0.2
Nov-07	1,936,825,843 ( $p_{1G} = 6.1$ )	<b>5636</b>	3970		$3.8 \pm 5.9$	Uni-Modal	0.5
Dec-07	3,880,906,219 ( $p_{1G} = 18.3$ )	<b>894</b>			$3.0 \pm 1.7$	Bi-modal	0.5, 2.2
Feb-08	15,322,558 ( $p_{1G} = 10$ )	<b>635</b>			$3.3 \pm 3.5$	Uni-modal	0.3
Apr-08	1,485,532,317 ( $p_{1G} = 16.3$ )	<b>3090</b>			$2.5 \pm 2.4$	Uni-modal	0.3
Apr-08 Outdoor	1,964,982,556 ( $p_{1G} = 6.4$ )	<b>617</b>			$3.7 \pm 5.7$	Uni-modal	0.2
May-08	109,324,893 ( $p_{1G} = p_{2G} = p_{3G} = 18.2$ )	6264 ( $p_{12} = 10.7$ ; $p_{13} = 12.9$ )	<b>20413</b> $p_{23} = 5.8$	463	$2.8 \pm 0.9$	Uni-modal	0.2
Aug-08	54,902,478 ( $p_{1G} = 17.2$ )	<b>9516</b>			$3.1 \pm 2.0$	Bi-modal	0.2, 0.5
Oct-08	28,364,545 ( $p_{1G} = 15.8$ )	<b>11029</b>			$4 \pm 5.4$	Bi-modal	0.2, 0.5
Nov-08	126,981,713 ( $p_{1G} = 17.3$ )	<b>9317</b>			$3.3 \pm 3.2$	Uni-modal	1
Dec-08	413,228,495 ( $p_{1G} = 32.4$ )	<b>10222</b>			$3.1 \pm 3.9$	Bi-modal	1, 1.4
Mar-09	433,206,931 ( $p_{1G} = 14.8$ )	<b>6429</b>			$3.5 \pm 4.3$	Uni-modal	0.3
Apr-09	743,385,334 ( $p_{1G} = 14.8$ )	<b>9368</b>			$2.5 \pm 2.4$	Uni-modal	0.3
Apr-09 Outdoor	1,785,799,623 ( $p_{1G} = 16.5$ )	<b>7226</b>			$3.7 \pm 5.7$	Uni-modal	1
May-09	1,105,039,043 ( $p_{1G} = 16.3$ )	<b>6353</b>			$3.9 \pm 7.5$	Uni-modal	0.3

Boldface figures show the numbers used for the calculations and discussion.

#### 2.4. Particle size and shape detection

The particle size and shape analyzer (Particle Analysis Tab, Genesis Software, US) was used. Roughly 500–1000 particles needed to be characterized to get a representative sample [18], depending on the sample complexity and the overall research objectives. More than 1000 particles per sample were analyzed using automated X-ray and morphology data from discreet grayscale features. The number of particles counted per sample is given in Table 1. To be analyzed accurately, the particles needed accurate grayscale contrast from the background and reasonable separation from each other. The analysis was conducted in an environmental mode to avoid any edge effects, charging, and variable background intensity. The image collected in the environmental mode showed better contrast between the particles and background, and gray level thresholds were calibrated for consistency and reproducibility. The resolution was chosen based on the size of the particles and the magnification used for analysis. The statistical tests for verifying the quality of the data were last used by Skogstad et al. [19].

At least 20 image fields were randomly selected on the filter paper. Particles were counted and characterized by automated analysis. The entire dataset was validated by testing for reproducibility by a Student-paired *t*-test. The hypothesis used was “there is no difference between the two data sets.” The hypothesis was tested at a 95% confidence level. The experiments were repeated one or two times to test the reproducibility of the data. The *p*-values are mentioned in this study in the following manner:

- $p_{12}$ : Student paired *t*-test between the first and second data set.
- $p_{13}$ : Student paired *t*-test between the first and third data set.
- $p_{23}$ : Student paired *t*-test between the second and third data set.
- $p_{1G}$ : Student paired *t*-test between the first and the GRIMM data set.
- $p_{2G}$ : Student paired *t*-test between the second and the GRIMM data set.
- $p_{3G}$ : Student paired *t*-test between the third and the GRIMM data set.

The GRIMM data sets have been published by Kadiyala and Kumar [20] and Kumar et al. [21]. These verified reproducible data sets are presented in this study and used for drawing the conclusions.

For this study, a line chart showing the size distribution was drawn and mode values were reported. The count and size distribution analyses were carried out on randomly selected observation fields. All particles within a field of view were counted and their

diameter and area (measured with the help of Genesis Software in real time with EDX) were tabulated. Tightly bound agglomerates were counted as single particles. Backscattered electron images were obtained for each particle and analysis field. The magnification for single particle images was adjusted based on particle size. The secondary and X-ray signals were collected in synchronization with the electron beam position to provide highly detailed spatial and compositional information of microscopic features. The SEM analysis showed that the samplers collected the intended size fractions and filters were evenly loaded. The particle shape factors were calculated by the formula published by Shandilya and Kumar [14]. According to software specifications, the aspect ratio (AR) was calculated using the following equation:

$$AR = \frac{\text{major axis}}{\text{minor axis}}$$

### 3. Results and discussion

#### 3.1. Size distribution

To evaluate the seasonal trend of the characteristics and size distribution of the PM, this study was carried out over 36 months. A total of 15 airborne PM samples distributed among five different urban-public transit buses (inside), fueled over 36 months by biodiesel blend, were collected (Table 1). The data collection was occasionally discontinued due to technical problems or maintenance issues.

The SEM/EDX coupled with Genesis Software in real time measured particle size collected on filter paper with each distribution plotted for each filter paper. The modality and peak found in the distribution are reported below in Table 1.

Size distribution for filter papers collected inside the biodiesel-fueled bus was mainly uni-modal for January and November 2007; February, April, May, and November 2008; March, April, and May 2009; while it was bi-modal for December 2007 and August, October, and December 2008. The PSD was found bi-modal in the winter and fall months; it was primarily uni-modal during spring and summer except August 2008. The modality of size distribution arises due to the particles coming from the different sources. The uni-modality of the particle size distribution suggests that particle collected and analyzed were originated from the same source. The point can be noted that salt is applied on the road in the winter and late fall months. These salt particles were found in the single particle chemical analysis on the filter paper [14]. The bi-modal distribution can be due to the presence of these particles. The primary

source contributing to the indoor air are infiltrated ambient air and passengers [20]. The size distribution found with the GRIMM monitor was uni-modal all the time with the peak below or at 0.3  $\mu\text{m}$ . The peaks in uni-modal distribution were found at 0.2, 0.3, 0.5 and 1  $\mu\text{m}$ . The peaks in bi-modal distribution were found at 0.2, 0.5, 1, 1.4 and 2.2  $\mu\text{m}$ . Uni-modal size distribution is a common phenomenon in urban aerosols in modern mega cities and times [8]. However, the uni-modal size distribution indicates the absence of particulates from many sources. This is attributed to the meteorological condition.

Almost all particles were found to be less than 20  $\mu\text{m}$ , which shows that the GRIMM sampler worked efficiently. The smaller peak in a particular size distribution shows the dominance of smaller particles. The peak for filter papers collected inside the biodiesel-fueled bus was found at a small particle size, so one could conclude that smaller particles dominate inside the biodiesel-fueled bus. The shape of the particles will be discussed in the next section, to explain the different modalities of particles deposited on filter papers collected inside the biodiesel-fueled bus.

The uni-modal and bi-modal peak lies in the ultrafine mode region. The ultrafine modes are seen to possess such a small, narrow size distribution (between 0.2 and 0.3  $\mu\text{m}$ ) that they cannot be formed directly from natural mineral particles, which are usually discrete grains larger than 1  $\mu\text{m}$  [8]. The well-established vaporization–condensation mechanism can explain the ultrafine mode formation [22].

The coarse modes around 1 or 2  $\mu\text{m}$  found in this study are clearly the consequence of the coalescence of bulk mineral matter present in the original particles. This is because the classical theory suggests that the vaporization–condensation mechanism cannot possibly produce such large particles [8]. These may possibly be mineral origin particles.

On the other hand, uni-modal and bi-modal PSD (generally found around  $\text{PM}_{0.1}$ ) corresponds to particles with long atmospheric residence times that are much less affected by short-term events and indoor–outdoor climate fluctuations. Many researchers have established the potential dangerous impact of these numerous small particles on human health [23]. While interpreting the results of this study, it must be noted that the susceptible people, viz. infants, are still more exposed because their respiratory systems are still developing and they breathe even more air per kilogram of body mass than adults [24]. These small particles generally originate from vehicular traffic. According to Granum and Lovik [25], the air PM persistence strengthens from a few hours to a few weeks from coarse to ultrafine particles, respectively, with an intermediate behavior for fine PM. Therefore, the lifetime of small particles in the atmosphere is long, and such particles can reside in the air for a long time. An explanation of the data is that the degree of PM air pollution in the biodiesel-fueled bus owes to the persistence of these small particles.

### 3.2. Particle shape analysis

The SEM/EDX-coupled with Genesis Software in real time was used to measure the dimensions of the particles. The shape factor distribution of the particles collected on the filter paper was calculated using the formula mentioned in Shandilya and Kumar [14]. Each particle shape factor distribution was plotted for each filter paper. Qualitative assessment of the images shows that most of the visible particles are composed of small chains and unidentifiable, roughly circular particles [14,15].

Scanning electron microscope (SEM) micrographs of the various shapes of the particles were shown in Shandilya and Kumar [14]. The angular particle shape indicates that there are several sharp angles on its surface. Meanwhile, the cubical shape shows smooth angles compared to the angular shape. An elongated particle is

characterized by a longer length than width of the particle. According to Bouwman et al. [26], the particle shape can be described based on the aspect ratio, Stokes's shape factor, and radial shape factor. The shape of the particle affects the settling, separation during flow, viscosity, and particle interactions. It is known that anisometric particles with a difference in length versus width are more dangerous than particles which have similar dimensions in length and width (isometric particle). This is because high surface areas will provide more contact area and, therefore, have a higher potential to absorb and interact with the gases and then affect the lung tissue. For example, particles in cubic shapes provide good penetration while elongated particles give superior penetration, reduce shrinkage and reduce thermal expansion of the particle. However, instead of the aspect ratio factor, other factors such as particle size, size distribution, and interfacial surface properties might also influence the properties of particulate matter.

Square particles existed in all samples and there were three kinds of square particles, as previously mentioned [14]. A cubical particle shows the smallest dimension of particle size while the angular shape has the largest dimension of particle size. The particle size is important since it affects the settling rate and thermal/optical properties. The square shaped particles were prevalent in all seasons and in all the samples. The most plausible explanation for this is that square shaped particles are characteristic of the air of Toledo, as explained in Shandilya and Kumar [14].

The surface of most oblong particles also had attached microspheres. These surfaces exhibited a crystalline morphology. Some were smooth while others were coarse, with the particle surface less smooth but containing holes or layered structures. The different vehicle and source types may be the main reason for the different particle types. A large amount of additional experimental data is needed to relate the particle type to the different sources. This information could help reduce the most dangerous types of particles.

The formation causes of different types of particulate matter are due to different mechanisms. Spherical particles are mostly formed after combustion. As the temperature decreases, mineral compounds (like heavy metals) condense onto tiny nuclei and grow to form spheres. Unburned carbon and mineral substances may be the main components of other geometrical-shaped particles. Further composition analysis may help deepen research on their real formation processes. Particle shapes result in a different particle exterior surface area-to-volume ratios and non-uniform heat fluxes in the particle, which can further affect the condensation and oxidation rates.

As for the particle shape, a spherical shape is usually assumed in modeling work for convenience. The characteristic dimension is taken as the spherical-equivalent diameter (a sphere diameter with the same volume/mass as the non-spherical particle). The particles can be classified according to their shapes and structures using SEM in 11 microstructure types: strip, oblong, triangle, square, pentagonal, hexagonal, heptagonal, octagonal, nonagonal, decagonal, and round particles.

The major fraction of the particles collected inside the urban-transit public bus fueled by biodiesel blend was either oblong or square-shaped. By observing the shape factor distribution, one can conclude that most particles were oblong in 2007, while most particles were square-shaped in 2008. The particle shape factor distribution in 2009 was mostly square in April and oblong in March and May.

By observing the shape factor distribution, one can conclude that most of the particles were square-shaped except in February 2008 (particle size distribution was uni-modal). Whenever the particle size distribution was bi-modal or there was the presence of coarse mode particles, the oblong-shaped particles were almost equal in number to the square particles. Shandilya and Kumar [14] reported



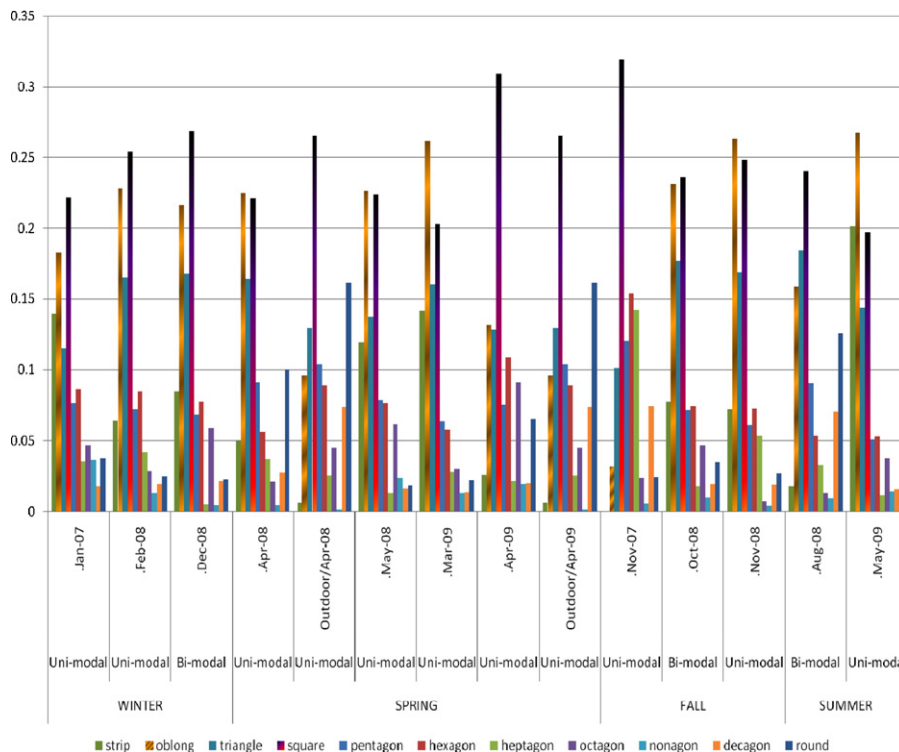


Fig. 2. Shape factor distributions and modality.

oblong particles rich in aluminosilicates (which may come from molten minerals). All the filters collected many of the smooth globular particles (referred to as round particle) approximately  $<2 \mu\text{m}$  in size, these may be derived from the vehicle combustion process. The SEM micrographs of the various particle shapes were shown previously [8]. The angular shape of any natural particle indicates that the shape has one or more sharp angles on its surface. The shape factor distribution for different months is given in Fig. 2.

Fused particles consist of various shapes such as heptagonal, pentagonal, and hexagonal, which are referred to as irregular shaped. High agglomeration is observed in the morphology of particles due to the autogenous breakage mechanism that allows particle breakage along the weak planes and minimizes surface energy. Unlike natural particles, the fused particles morphology shows agglomeration.

When the PSD is uni-modal or bi-modal, the oblong particles are prevalent in the sample; when the PSD is multi-modal, the square particles are prevalent in the sample. Particle shape affects the settling, separation during flow, viscosity, and particle dynamics. Anisometric particles with difference in length versus width are more likely to agglomerate than particles having similar dimensions in length and width (isometric particle). This is because the high surface area will provide more contact area and, therefore, will have a higher potential to reinforce the matrix.

### 3.3. Aspect ratio

The aspect ratio for elongated particles is more than one. The shape of particles of the low or high aspect ratio may affect the properties of the particles. The description, based on aspect ratio, is commonly being used by many researches when dealing with shape factor [27]. The aspect ratio found for different filters collected inside the bus fueled by the biodiesel blend were in the average value range of 2.4–3.6, while the standard deviation value ranged 0.9–7.4. Particles from various parts of a filter show different morphologies that are dependent on the different formation

mechanism. This is associated with an increasing aspect ratio (width/length) for the aggregates. The variation in the aspect ratio can be explained by taking two cases. Suppose in one case measurements in various samples show that the length ranges from 100 to 300 nm, the largest percentage with a length of 40 nm. Therefore, the variation in width is responsible for the variation in ratio. The second case can be made vice versa. A big variation in aspect ratio indicates that variation in both length and width are responsible. Generally, particles with long width result in large aspect ratio and vice versa.

An elongated particle is characterized by a length longer than the width of the particle (i.e. high aspect ratio  $>1$ ). Elongated particles dominate the indoor environment of both the buses. The variation of aspect ratio is still unexplainable and needs further investigation. The aerosol mixtures inside both buses are dynamic in nature. According to Bouwman et al. [26], the particle shape can be described based on the aspect ratio, Stokes's shape factor, and radial shape factor. In this study, the aspect ratio of particles was calculated based on the number of particles counted using SEM micrographs with the help of Genesis Software. Fig. 3 shows the aspect ratio average for different samples. Clearly the aspect ratio of all the particles was usually in the range of 2.5, though the standard deviation varied greatly. It is believed that particle aspect ratios and shapes do not change as dynamically as size during condensation. The non-spherical nature of the particles increases with larger size and aspect ratios.

While interpreting these results, some facts need to be kept in mind. Both triangle and plates have higher surface-area-to-mass ratios than rounds (in three dimensions), and the difference is more obvious with an increasing aspect ratio. A high aspect ratio provides a high surface area, which results in more contact area between the particles for agglomeration and reaction. By good adhesion between particles, a positive reinforcement effect occurs in elongated particles, which may strengthen those particles as the elongated particle shape has a higher particle surface resulting in more contact area between the particles. This agglomeration prop-

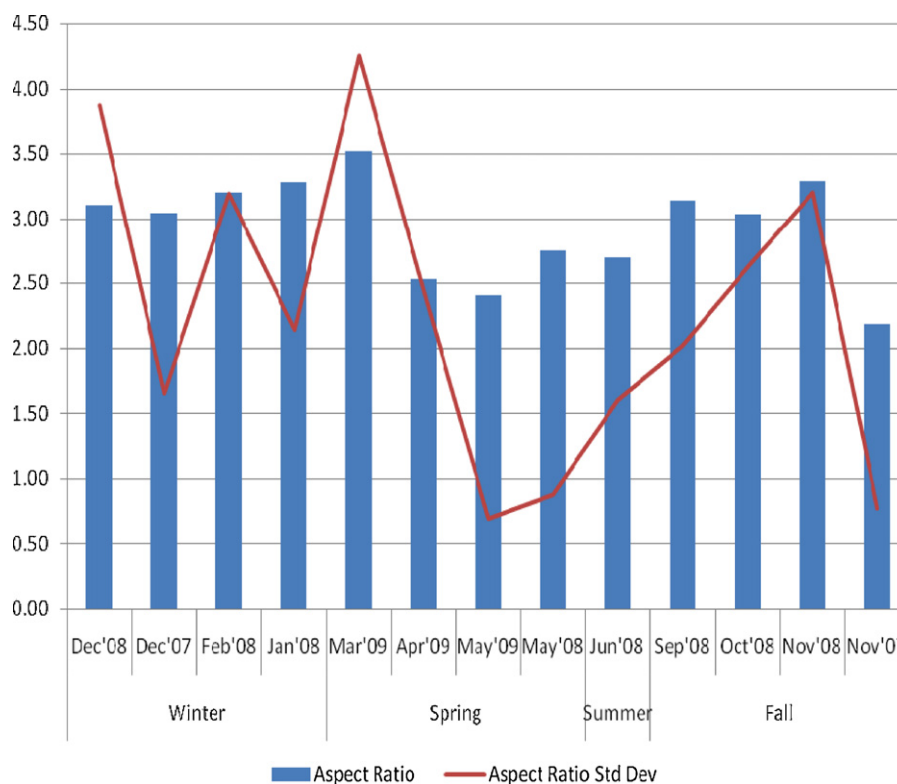


Fig. 3. Aspect ratio and standard deviation of particles.

erty shows a permanent bonding of particles during their flow in the environment. Both cylinders and plates have higher surface-area-to-mass ratios than spheres, and the difference is clearer with a larger aspect ratio.

#### 4. Conclusion

In this study we compared the physical characteristics of fine particulates collected inside urban-public transit buses in Toledo that run on B20. The physical characterization of fine particulates is conducted in terms of particle number size distribution, microstructure, and aspect ratio. The fine PM filter samples were collected inside these transit buses and were analyzed using an ESEM/EDX for three years (2007, 2008, and 2009). The size distribution was generally uni-modal for the B20-fueled bus. The size distribution multi-modality may be due to the agglomeration or presence of other sources. The aspect ratio found for different filters collected inside the bus fueled by the B20 blend was in the average value range of 2.4–3.6 with a standard deviation range of 0.9–7.4. The square and oblong-shaped particles represented the single inhalable particle's morphology characteristics in the air of a Toledo transit bus. The major limitation of this study had to consider the agglomerate as a group of floccules, spherules, and agglomerates. The authors are working on this limitation, and the future research direction is composition analysis that can help deepen research on the real formation process inside the bus. Researchers may want to use the shape factor found here for the calculations for particle number to mass conversion.

#### Acknowledgements

The authors would like to thank the Michigan-Ohio University Transit Consortium, United States Department of Transportation (US DOT), and Toledo Area Regional Transit Authority (TARTA) for the alternate fuel grants awarded to the Intermodal Transportation

Institute (ITI) of The University of Toledo. The authors would also like to express their sincere gratitude to the TARTA management and the employees for their continued interest and involvement in this research. The authors are also thankful to Electronic Microbeam Analysis Laboratory facility of Space Research Center at The University of Michigan for letting us use their facility for research. The views expressed in this study are those of the authors alone and do not represent the views of the funding organizations. The authors would like to thank Mr. Dinesh Chandra Somuri (MS student) for providing filter papers for analysis and Mr. Tom Zallocco for providing miscellaneous help.

#### References

- [1] J.H. Park, J.D. Spengler, D.W. Yoon, T. Dumyahn, K. Lee, H. Ozkaynak, Measurement of air exchange rate of stationary vehicles and estimation of in-vehicle exposure, *Journal of Exposure Analysis and Environmental Epidemiology* 8 (1) (1998) 65–78.
- [2] J.S. Lighty, J.M. Veranth, A.F. Sarofim, Combustion aerosols: factors governing their size and composition and implications to human health, *Journal of the Air & Waste Management Association* 50 (9) (2000) 1565–1618.
- [3] C. Perrino, Atmospheric particulate matter, in: *Proceedings of a C.I.S.B. Minisymposium—March, 2010*, pp. 35–43.
- [4] A. Lall, X. Ma, S. Guha, G.W. Mulholland, M.R. Zachariah, Online nanoparticle mass measurement by combined aerosol particle mass analyzer and differential mobility analyzer: comparison of theory and measurements, *Aerosol Science and Technology* 43 (11) (2009) 1075–1083.
- [5] C.H. Twohy, S.M. Kreidenweis, T. Eidhammer, E.V. Browell, A.J. Heymsfield, A.R. Bansemer, B.E. Anderson, C. Gao, S. Ismail, P.J. Demott, S.C. Van Den Heever, Saharan dust particles nucleate droplets in eastern Atlantic clouds, *Geophysical Research Letters* 36 (February (1)) (2009) 6.
- [6] M. Lippmann, L. Chen, Health effects of concentrated ambient air particulate matter (CAPs) and its components, *Critical Reviews in Toxicology* 39 (10) (2009) 865–913.
- [7] J. Pauluhn, Comparative pulmonary response to inhaled nanostructures: considerations on test design and endpoints, *Inhalation Toxicology* 21 (s1) (2009) 40–54.
- [8] K.K. Shandilya, M. Khare, A.B. Gupta, Defining aerosols by physical and chemical characteristics, *Indian Journal of Air Pollution Control* IX (March (1)) (2009) 107–126.

- [9] L. Morawska, S. Thomas, M. Jamriska, G. Johnson, The modality of particle size distributions of environmental aerosols, *Atmospheric Environment* 33 (27) (1999) 4401–4411.
- [10] K. Wittmaack, In search of the most relevant parameter for quantifying lung inflammatory response to nanoparticle exposure: particle number, surface area, or what? *Environmental Health Perspectives* 115 (2) (2007) 187–194.
- [11] A Korolev, G. Isaac, Roundness and aspect ratio of particles in ice clouds, *Journal of the Atmospheric Sciences* 60 (15) (2003) 1795–1808.
- [12] H.M. Ortner, P. Hoffmann, S. Weinbruch, F.J. Stadermann, M. Wentzel, Chemical characterization of environmental and industrial particulate samples, *The Analyst* 123 (5) (1998) 833–842.
- [13] T.L. Conner, G.A. Norris, M.S. Landis, R.W. Williams, Individual particle analysis of indoor, outdoor, and community samples from the 1998 Baltimore particulate matter study, *Atmospheric Environment* 35 (23) (2001) 3935–3946.
- [14] K.K. Shandilya, A. Kumar, Morphology of single inhalable particle inside public transit biodiesel fueled bus, *Journal of Environmental Sciences* 22 (2) (2010) 263–270.
- [15] K.K. Shandilya, A. Kumar, Qualitative evaluation of particulate matter inside public transit buses operated by biodiesel, *The Open Environmental Engineering Journal* 3 (2010) 13–20.
- [16] <http://smartech.gatech.edu/bitstream/1853/22231/1/wp37.pdf> (accessed in 2009).
- [17] M.S. Germani, P.R. Buseck, Automated scanning electron microscopy for atmospheric particle analysis, *Analytical Chemistry* 63 (1991) 2232–2237.
- [18] Y. Mamane, R.D. Willis, T.L. Conner, Evaluation of computer-controlled scanning electron microscopy applied to an ambient urban aerosol sample, *Aerosol Science Technology* 34 (2000) 97–107.
- [19] A. Skogstad, L. Madsø, W. Eduard, Classification of particles from the farm environment by automated sizing, counting and chemical characterization with scanning electron microscopy–energy dispersive spectroscopy, *Journal of Environmental Monitoring* 1 (1999) 379–382.
- [20] A. Kadiyala, A. Kumar, Application of CART and Minitab software to identify variables affecting indoor concentration levels, *Environmental Progress* 27 (2) (2008) 160–168.
- [21] A. Kumar, A. Kadiyala, V.V.K. Nerella, K.K. Shandilya, S. Velagapudi, D. Somuri, Characterization of emissions and indoor air quality of public transport buses using biodiesel and ultra-low sulfur diesel, in: *Proceedings of the International Conference on Emerging Technologies in Environmental Science and Engineering*, October 26–28, Aligarh Muslim University, Aligarh, India, 2009.
- [22] F. Yu, R.P. Turco, Ultrafine aerosol formation via ion mediated nucleation, *Geophysical Research Letters* 27 (6) (2000) 883–886.
- [23] J. Schwartz, Air pollution and children's health, *Pediatrics* 113 (2004) 1037–1043.
- [24] H.L. Sun, M.C. Chou, K.H. Lue, The relationship of air pollution to ED visits for asthma differ between children and adults, *American Journal of Emergency Medicine* 24 (6) (2006) 709–713.
- [25] B. Granum, M. Lovik, The effect of particles on allergic immune responses, *Toxicological Sciences* 65 (2002) 7–17.
- [26] A.M. Bouwman, J.C. Bosma, P. Vonk, J.A. Wesselingh, H.W. Frijlink, Which shape factor(s) best describe granules? *Powder Technology* 146 (2004) 66–72.
- [27] W. Pabst, C. Berthold, E. Gregorova, Size and shape characterization of poly-disperse short-fiber systems, *Journal of European Ceramic Society* 26 (2005) 149–160.